JOURNAL OF COMPUTATIONAL PHYSICS 105, 150-164 (1993)

The Treatment of Spurious Pressure Modes in Spectral Incompressible Flow Calculations

TIMOTHY N. PHILLIPS AND GARETH W. ROBERTS*

Department of Mathematics, University of Wales, Aberystwyth, Aberystwyth SY23 3BZ, United Kingdom

Received December 5, 1990; revised June 10, 1992

Algorithms for the transient and steady state simulation of incompressible Newtonian and non-Newtonian flows are described for the primitive variable formulation of the governing equations. Spectral approximations are used for the spatial discretization. Attention is given to the satisfaction of the incompressibility constraint and the determination of the pressure. Spurious pressure modes are removed by means of a singular value decomposition. The corresponding velocity field is divergence free at all the collocation points. Numerical results are presented for Newtonian flow in a regularized driven square cavity and for non-Newtonian flow in a planar channel and in a journal bearing for a realistic range of material parameters.

1. INTRODUCTION

The time-dependent incompressible Navier–Stokes equations in primitive variable form are usually written as

$$\frac{\partial \mathbf{v}}{\partial t} + \mathbf{v} \cdot \nabla \mathbf{v} = -\nabla p + \nu \nabla^2 \mathbf{v}, \tag{1}$$

$$\nabla \cdot \mathbf{v} = 0, \tag{2}$$

where $\mathbf{v} = (u, v)$ is the velocity vector, p is the pressure, and ν the kinematic viscosity. Equations (1) and (2) are the mathematical statements of the conservation of momentum and mass, respectively. We sometimes refer to (2) as the continuity equation or the incompressibility constraint. These equations are solved in a domain Ω subject to velocity boundary conditions and initial conditions of the form

$$\mathbf{v}(\mathbf{x}, 0) = \mathbf{v}_0(\mathbf{x}) \qquad \text{in } \Omega. \tag{3}$$

It is important that the initial velocity field is divergence-free; otherwise the continuous problem does not possess a classical solution (Heywood and Rannacher [18]). Furthermore, this field needs to be compatible with the momentum equation (1) to avoid singularities at the initial time (Deville *et al.* [11]). In the general case, however, singularities in the tangential velocity component on no-slip walls at the initial time are unavoidable and vortex sheets are the result (Gresho [15]). The numerical algorithm does not generally need to be designed to have sufficient damping properties to handle the initial singularities during the beginning of the time-integration process since the viscous term, which is the physical damping mechanism, is sufficient to properly smooth them out. For this reason it is not necessary to add additional dissipation to the numerical algorithm and so the trapezoidal rule may be used, for example.

The main difficulty in solving these equations numerically is the treatment of the pressure. Unlike the velocity variables there is no evolution equation for the pressure. Instead it is determined by the incompressibility constraint (2). In fact the pressure may be viewed as a Lagrange multiplier which ensures that the flow is divergence-free. Penalty methods, sometimes known as artificial compressibility methods, circumvent this difficulty by adding a false pressure time-derivative into the continuity equation (Chorin [8], Temam [31], Yanenko [32]). The idea underlying the method is to consider the solution of the steady equations as the limit as $t \to \infty$ of the solution of the unsteady equations in which the continuity equation is perturbed to obtain a system of evolution equations which can be easily solved by standard numerical techniques. Chorin [8] writes the perturbed equation in the form

$$\frac{\partial p}{\partial t} + c^2 \nabla \cdot \mathbf{v} = 0,$$

where c is a constant chosen to ensure the convergence of the system to the steady state solution. The method can be

* Present address: School of Mathematics, University of Wales, Bangor, Dean Street, Bangor LL57 1UT, UK.

0021-9991/93 $5.00

termed a pseudo-unsteady method since the time t has no physical significance. Furthermore, the incompressibility constraint is only satisfied when the steady state is reached and therefore is inadequate for reliable transient simulations. Fortin, Peyret, and Temam [13] show that the exact solution of the unsteady Stokes problem converges to the solution of the steady Stokes problem.

The formulation of the Poisson equation for the pressure is the main alternative to the penalty method and represents the mode of pressure determination that is most widely used in finite difference and spectral simulations of incompressible flows. If we take the divergence of (1) and impose (2) we obtain the Poisson equation

$$\nabla^2 p = -\nabla \cdot (\mathbf{v} \cdot \nabla \mathbf{v}). \tag{4}$$

The pressure problem is well posed if we have one condition specified on $\partial\Omega$, the boundary of Ω. However, at a no-slip boundary $\mathbf{v} = 0$ and therefore (1) reduces to

$$\nabla p = \nu \nabla^2 \mathbf{v}. \tag{5}$$

In three dimensions this implies that the three derivatives of p are known on the no-slip part of the boundary $\partial\Omega$. Despite this apparent over-specification, (4) and (5) do have a unique solution since the source term on the right-hand side of (4) is not arbitrary but a function of the velocity components. Thus if $\mathbf{v}$ and p evolve together then (4) and (5) will remain soluble.

We still need to decide which pressure derivative condition to use in the numerical simulation. For inviscid flow there is no problem since $\mathbf{v} \cdot \mathbf{n} = 0$ on $\partial\Omega$ and therefore only the normal component of (5) is valid. However, for viscous flow both Dirichlet and Neumann conditions may be specified for the pressure if $\mathbf{v}$ is known. It is important that the solution procedure is designed so that $\mathbf{v}$ and p remain consistent with the over-specified pressure equation. Gresho and Sani [14] show that if velocity boundary conditions are prescribed then the proper choice of boundary condition for (4) is to apply the normal component of (5) since this is the only condition that can always assure that $\nabla \cdot \mathbf{v} = 0$ in Ω. Orszag, Israeli, and Deville [23] describe a number of different algorithms for implementing no-slip boundary conditions in order to achieve high-order accurate time integrations of the incompressible flow equations.

In this paper we consider implicit and explicit splitting schemes for solving a one-dimensional Stokes problem which is a linear model that encapsulates two essential features of the Navier–Stokes equations, namely, incompressibility and pressure determination. The techniques proposed in this paper for the treatment of incompressibility and pressure may be incorporated into more general algorithms for solving the full Navier–Stokes equations or the governing equations of non-Newtonian flow. A projection method is used to ensure that the velocity field is divergence-free at the end of each time-step. This type of splitting technique was first proposed by Chorin [9]. The need for intermediate velocity boundary conditions is alleviated by means of an algorithm of Ku, Taylor, and Hirsh [21]. This is a generalization to spectral approximations of a technique originally devised by Peyret and Taylor [24] for finite difference discretizations. The technique uses the continuity equation at interior and boundary nodes, or collocation points, to obtain a system of algebraic equations for the pressure unknowns without explicit imposing a pressure boundary condition. Spurious pressure modes are eliminated by seeking a solution for the pressure in a suitably defined subspace of $\mathcal{P}_N$, the space of algebraic polynomials of degree less than or equal to N, which is orthogonal to the space spanned by these modes. This is facilitated by means of a singular value decomposition (SVD) in which rows of the system that correspond to zero singular values are replaced by the algebraic conditions which set these modes to zero. The velocity field at the end of the projection step is then divergence-free and satisfies the no-slip boundary conditions. An extension of this algorithm to solve non-Newtonian flows is described. Several examples are considered illustrating the convergence properties of the scheme.

The technique that we develop in this paper is computationally efficient particularly when used to solve time-dependent problems. Since the coefficient matrix for the pressure problem remains unchanged at each time step the SVD of this matrix needs to be computed only once in a pre-processing step before the time-stepping commences. The inverse of the SVD of this coefficient matrix is easy to compute since it involves the multiplication of two orthogonal matrices. This inverse is then stored and used to calculate the pressure at each time step. The SVD requires about $10n^3$ floating point operations (flops), where n is the order of the matrix. To find the pressure at each time step we require a matrix–vector multiplication which is an $O(n^2)$ operation. A similar number of flops are required in the implementation of the influence matrix technique (see [19], for example). However, that method requires far more storage than the method proposed in this paper since the solutions to $O(n^{1/2})$ Stokes problems need to be stored from a pre-processing stage. Further, the influence matrix method produces a velocity approximation which is identically divergence-free only at the boundary collocation points. In contrast the velocity approximation in the method we propose satisfies the continuity equation exactly at all the collocation points at each time step and for cartesian geometries it satisfies this equation globally.

2. A MODEL STOKES PROBLEM

The Stokes problem represents a model which possesses the same computational difficulties as the Navier–Stokes

equations in terms of satisfaction of the continuity equation and the determination of the pressure. Therefore in order to simplify the details we describe implicit and explicit splitting schemes for a model Stokes problem. The generalization of the method to the Navier–Stokes equations is relatively straightforward and will be discussed later.

Consider the 2D Stokes problem in the infinite slab $-\infty < y < \infty$, $|x| \leqslant 1$. The governing flow equations are

$$\frac{\partial \mathbf{v}}{\partial t} = -\nabla p + \nu \nabla^2 \mathbf{v}, \tag{6}$$

$$\nabla \cdot \mathbf{v} = 0, \tag{7}$$

subject to no-penetration and no-slip boundary conditions at $x = \pm 1$. If we assume periodicity in the y-direction both $\mathbf{v}$ and p may be decomposed into their Fourier modes:

$$\begin{aligned} \mathbf{v}(\mathbf{x}, t) &= \sum_{k=-\infty}^{\infty} \mathbf{v}^k(x, t)\, e^{iky}, \\ p(\mathbf{x}, t) &= \sum_{k=-\infty}^{\infty} p^k(x, t)\, e^{iky}. \end{aligned} \tag{8}$$

Let us examine one particular mode and define

$$\begin{aligned} \mathbf{v}(\mathbf{x}, t) &= \mathbf{v}^k(x, t)\, e^{iky}, \\ p(\mathbf{x}, t) &= p^k(x, t)\, e^{iky}. \end{aligned} \tag{9}$$

The complete solution may be found by the principle of linear superposition of solutions. If we insert (9) into (6) and (7) we obtain the equations

$$\frac{\partial u}{\partial t} = -\frac{\partial p}{\partial x} + \nu \left(\frac{\partial^2 u}{\partial x^2} - k^2 u \right), \tag{10}$$

$$\frac{\partial v}{\partial t} = kp + \nu \left(\frac{\partial^2 v}{\partial x^2} - k^2 v \right), \tag{11}$$

$$\frac{\partial u}{\partial x} + kv = 0, \tag{12}$$

where $u = u^k$, $v = iv^k$, and $p = p^k$. We describe numerical schemes for solving (10)–(12).

3. TIME SPLITTING SCHEMES

This class of numerical method was originally devised for the incompressible Navier–Stokes equations by Chorin [9] and Temam [30]. The basic idea is to decouple the pressure and velocity computations at each time step. The terms on the right-hand sides of (10) and (11) are computed at the old, new, or some intermediate time. Implicit treatments of these terms enable larger time steps to be taken but require the solution of a boundary-value problem at each time step. On the other hand, explicit methods are easier to code and require less computational work per time step but suffer from severe time step restrictions in order to preserve the stability of the scheme.

We first examine a fully implicit scheme for solving (10)–(12):

IMPLICIT SCHEME. *Stage* A.

$$\frac{u^* - u^n}{\Delta t} = -\frac{\partial p^n}{\partial x}, \tag{13}$$

$$\frac{v^* - v^n}{\Delta t} = kp^n, \tag{14}$$

$$\frac{\partial u^*}{\partial x} + kv^* = 0, \tag{15}$$

$$u^*(\pm 1) = 0; \tag{16}$$

Stage B.

$$\frac{u^{n+1} - u^*}{\Delta t} = \nu \left(\frac{\partial^2 u^{n+1}}{\partial x^2} - k^2 u^{n+1} \right), \tag{17}$$

$$\frac{v^{n+1} - v^*}{\Delta t} = \nu \left(\frac{\partial^2 v^{n+1}}{\partial x^2} - k^2 v^{n+1} \right), \tag{18}$$

$$u^{n+1}(\pm 1) = v^{n+1}(\pm 1) = 0. \tag{19}$$

The condition (15) in Stage A implies that the pressure at the nth time step satisfies the Helmholtz equation

$$\frac{\partial^2 p^n}{\partial x^2} - k^2 p^n = \frac{1}{\Delta t} \nabla \cdot \mathbf{v}^n. \tag{20}$$

Gottlieb and Orszag [17] argue that only the normal velocity component can be specified at the boundary in Stage A since this part of the splitting scheme effectively deals with the inviscid part of the calculations at each time step. The condition $u^* = 0$ at $x = \pm 1$ implies homogeneous Neumann boundary conditions for p^n:

$$\frac{\partial p^n}{\partial x}(\pm 1) = 0. \tag{21}$$

At the end of Stage A the flow is divergence-free in the interior of the domain but there is a non-zero slip or tangential velocity that is $O(\Delta t)$. The magnitude of this slip velocity may be reduced to $O(\Delta t^3)$ by a judicious choice of the intermediate boundary condition on $\mathbf{v}^*$ [7]. In Stage B, the viscous part of the calculation, no-slip boundary conditions are imposed on the velocity field but $\mathbf{v}^{n+1}$ does not satisfy the incompressibility constraint. The failure to satisfy

this constraint can lead to numerical instability because mass is not conserved numerically.

The influence matrix or Green's function technique [19, 20, 7] may be used to obtain the correct pressure boundary conditions necessary to satisfy the continuity equation exactly in the discretized problem. The solution procedure is based on the fact that the continuity equation is equivalent to the Helmholtz problem for the pressure (20) with zero right-hand side and the satisfaction of the incompressibility condition on the boundary. In a pre-processing step the solutions to a number, N, of steady Stokes problems with linearly independent boundary values are found, where N is the number of collocation points on the boundary. The solution at the end of each time step is corrected by adding a linear combination of these N solutions. The coefficients in this linear combination are chosen so that the corrected velocity field satisfies the continuity equation at the boundary collocation points. The coefficient matrix of this system, known as the influence matrix, or its inverse, is calculated and stored for subsequent use before the time-integration process begins. This process is expensive in two or three dimensions in terms of the amount of memory required since the solutions to N steady Stokes problems need to be stored as well as the influence matrix or its inverse.

Farcy and Alziary de Roquefort [12] propose a similar method for the pseudospectral approximation of the incompressible Navier–Stokes equations. Their influence matrix is global and is based on both the boundary and interior collocation points. They approximate the full influence matrix by a truncated one which has five non-zero diagonals because of the high cost of storing and inverting the original matrix. An iterative method must then be used at each time step to ensure that the incompressibility constraint is adequately satisfied.

An alternative is the following explicit scheme for solving (10)–(12):

EXPLICIT SCHEME. *Stage* A.

$$\frac{u^* - u^n}{\Delta t} = \nu\left(\frac{\partial^2 u^n}{\partial x^2} - k^2 u^n\right), \tag{22}$$

$$\frac{v^* - v^n}{\Delta t} = \nu\left(\frac{\partial^2 v^n}{\partial x^2} - k^2 v^n\right); \tag{23}$$

Stage B.

$$\frac{u^{n+1} - u^*}{\Delta t} = -\frac{\partial p^n}{\partial x}, \tag{24}$$

$$\frac{v^{n+1} - v^*}{\Delta t} = kp^n, \tag{25}$$

$$\frac{\partial u^{n+1}}{\partial x} + kv^{n+1} = 0, \tag{26}$$

$$u^{n+1}(\pm 1) = 0, \tag{27}$$

$$v^{n+1}(\pm 1) = 0. \tag{28}$$

In this scheme Stage A represents the viscous part of the calculation. In Stage B a divergence-free velocity field is found satisfying the no-slip boundary conditions.

Strictly speaking, the introduction of the intermediate velocity $\mathbf{v}^*$ is not necessary as the viscous term could easily be incorporated into Stage B, thus merging the two stages into one. The advantage of retaining $\mathbf{v}^*$ occurs when we proceed to consider schemes for Navier–Stokes and non-Newtonian flows. The differences occur in Stage A only, leaving Stage B unchanged, thus simplifying both the presentation and computation. The condition (26) in Stage B implies that the pressure satisfies the Helmholtz equation

$$\frac{\partial^2 p^n}{\partial x^2} - k^2 p^n = \frac{1}{\Delta t}\nabla \cdot \mathbf{v}^*. \tag{29}$$

In this scheme the choice of pressure boundary conditions for (29) is crucial in order to obtain a divergence-free velocity field at the end of each time step. The degree to which the incompressibility constraint is satisfied depends on the spatial discretization.

4. DERIVATION OF THE DISCRETE PRESSURE PROBLEM

Ku, Taylor, and Hirsh [21] suggest a method which avoids the need to specify intermediate velocity boundary conditions and Neumann conditions for the pressure in the explicit scheme (22)–(28). The values of the intermediate velocity components u^* and v^* at the boundaries are eliminated from the algebraic system of equations for the values of the pressure at the collocation points and the system is closed by applying the continuity equation at the boundary. The velocity field at the end of the full time step is divergence-free at all boundary and interior collocation points and satisfies the no-slip boundary conditions.

The Chebyshev–Gauss–Lobatto points are given by

$$x_j = \cos(\pi j/N). \tag{30}$$

Note that $x_0 = 1$, $x_N = -1$ and that the interior points x_j, $1 \leqslant j \leqslant N-1$, are the zeros of $T'_N(x)$, where $T_N(x)$ is the Chebyshev polynomial of degree N. The Chebyshev polynomials are orthogonal with respect to the weight function $(1-x^2)^{-1/2}$ on the interval $[-1, 1]$ and are given explicitly

by $T_n(x)=\cos(n\cos^{-1}(x))$. Let f_j denote the value of a function $f(x)$ at the point x_j. The polynomial $f_N(x)$ which interpolates these values at the $N+1$ points x_j, $0\leqslant j\leqslant N$, is given by

$$f_N(x)=\sum_{n=0}^{N}\hat{f}_n T_n(x), \tag{31}$$

where the expansion coefficients are defined in terms of the f_j by

$$\hat{f}_n=\frac{2}{Nc_n}\sum_{j=0}^{N}\frac{f_j}{c_j}\cos\left(\frac{nj\pi}{N}\right), \tag{32}$$

where

$$c_j=\begin{cases}2 & \text{if } j=0, N,\\ 1 & \text{if } 1\leqslant j\leqslant N-1.\end{cases}$$

The derivative of $f_N(x)$ at $x=x_j$ is given by

$$f'_N(x_j)=\sum_{k=0}^{N}D_{j,k}f_k, \tag{33}$$

where D is the Chebyshev collocation differentiation matrix. The matrix D is full and its entries are given by

$$D_{j,k}=\begin{cases}\dfrac{c_j(-1)^{j+k}}{c_k(x_j-x_k)}, & j\neq k,\\ -\dfrac{x_k}{2(1-x_k^2)}, & 1\leqslant j=k\leqslant N-1,\\ \dfrac{2N^2+1}{6}, & j=k=0,\\ -\dfrac{2N^2+1}{6}, & j=k=N.\end{cases}$$

See Solomonoff and Turkel [29] for the derivation of these entries.

Let q_j^n denote the approximation to a variable q at the point x_j at the nth time step. If all the variables are expanded in terms of a truncated series of Chebyshev polynomials of the form (31) then the collocation equations for the projection step of the explicit scheme (Stage B) may be written in the form

$$u_j^{n+1}=u_j^*-\Delta t\sum_{m=0}^{N}D_{j,m}p_m, \qquad 1\leqslant j\leqslant N-1, \tag{34}$$

$$v_j^{n+1}=v_j^*+\Delta t\, kp_j, \qquad 1\leqslant j\leqslant N-1, \tag{35}$$

$$\sum_{i=0}^{N}D_{j,i}u_i^{n+1}+kv_j^{n+1}=0, \qquad 0\leqslant j\leqslant N, \tag{36}$$

$$u_0^{n+1}=u_N^{n+1}=0, \tag{37}$$

$$v_0^{n+1}=v_N^{n+1}=0. \tag{38}$$

Equations (34)–(38) are $3(N+1)$ equations for the $3(N+1)$ velocity and pressure unknowns. We substitute for u_i^{n+1} and v_j^{n+1} in (36) using (34), (35), (37), and (38). This yields the following system of equations:

$$\Delta t\left(\sum_{i=1}^{N-1}D_{j,i}\sum_{m=0}^{N}D_{i,m}p_m-k^2p_j\right)=D_{j,0}u_0^{n+1}+D_{j,N}u_N^{n+1}+\sum_{i=1}^{N-1}D_{j,i}u_i^*+kv_j^*, \qquad 1\leqslant j\leqslant N-1, \tag{39}$$

$$\Delta t\sum_{i=1}^{N-1}D_{0,i}\sum_{m=0}^{N}D_{i,m}p_m=D_{0,0}u_0^{n+1}+D_{0,N}u_N^{n+1}+kv_0^{n+1}+\sum_{i=1}^{N-1}D_{0,i}u_i^*, \tag{40}$$

$$\Delta t\sum_{i=1}^{N-1}D_{N,i}\sum_{m=0}^{N}D_{i,m}p_m=D_{N,0}u_0^{n+1}+D_{N,N}u_N^{n+1}+kv_N^{n+1}+\sum_{i=1}^{N-1}D_{N,i}u_i^*. \tag{41}$$

Equations (39)–(41) represent a system of $N+1$ linear equations for the unknown pressure values at the collocation points. When $k=0$ this system has rank $N-1$; otherwise it has rank $N+1$. The rank deficiency is due to the presence of spurious pressure modes. These will be defined in the next section, together with a technique for solving the system for $k=0$.

We can show that the above system is consistent with a discretization of the pressure Poisson equation (PPE) subject to a Neumann boundary condition derived from the normal momentum equation [14]. Let us examine (39), for example. If we substitute for the intermediate velocity variables in (39) using Stage A of the explicit scheme and rearrange the resulting equation we arrive at the formula

$$\Delta t\left(\sum_{i=1}^{N-1}D_{j,i}\sum_{m=0}^{N}D_{i,m}p_m-k^2p_j\right)=\left[D_{j,0}u_0^{n+1}+D_{j,N}u_N^{n+1}+\sum_{i=1}^{N-1}D_{j,i}u_i^n+kv_j^n\right]+\nu\,\Delta t\sum_{i=1}^{N-1}D_{j,i}\left(\frac{\partial^2u^n}{\partial x^2}-k^2u^n\right)_i+\nu\,\Delta t\left(\frac{\partial^2v^n}{\partial x^2}-k^2v^n\right)_j, \qquad 1\leqslant j\leqslant N-1.$$

Now consistent with forward Euler, use $u_0^{n+1}=u_0^n+\Delta t\,\dot{u}_0^n$

and $u_N^{n+1} = u_N^n + \Delta t\, \dot{u}_N^n$; then the first term on the right-hand side is thus

$$\Delta t(D_{j,0}\dot{u}_0^n + D_{j,N}\dot{u}_N^n) + \sum_{i=0}^{N} D_{j,i}u_i^n + kv_j^n.$$

Since $\nabla \cdot \mathbf{v}^n = 0$ this reduces to

$$\Delta t(D_{j,0}\dot{u}_0^n + D_{j,N}\dot{u}_N^n).$$

Thus the final discrete PPE is

$$\begin{aligned}\left(\sum_{i=0}^{N} D_{j,i} \sum_{m=0}^{N} D_{i,m}p_m - k^2 p_j\right) &= D_{j,0}\left(\dot{u}_0^n + \sum_{m=0}^{N} D_{0,m}p_m - \nu\left(\frac{\partial^2 u^n}{\partial x^2} - k^2 u^n\right)_0\right) \\ &+ D_{j,N}\left(\dot{u}_N^n + \sum_{m=0}^{N} D_{N,m}p_m - \nu\left(\frac{\partial^2 u^n}{\partial x^2} - k^2 u^n\right)_N\right) \\ &+ \nu \sum_{i=0}^{N} D_{j,i}\left(\frac{\partial^2 u^n}{\partial x^2} - k^2 u^n\right)_i \\ &+ \nu\left(\frac{\partial^2 u^n}{\partial x^2} - k^2 v^n\right)_j, \qquad 1 \leqslant j \leqslant N-1.\end{aligned}$$

The terms in brackets are approximations to the normal momentum equations at the boundaries $x = \pm 1$. Similar equations are obtained for $j = 0$ and $j = N$. Thus the system (39)–(41) corresponds to the discrete PPE and the proper boundary condition for the PPE. Note that since spectral methods yield global approximations each of the discrete equations is influenced by the boundary conditions.

5. TREATMENT OF SPURIOUS PRESSURE MODES

Let $p_N(x)$ be defined by

$$p_N(x) = \sum_{n=0}^{N} \hat{p}_n T_n(x); \tag{42}$$

then the spurious modes are defined to be those non-constant modes $T_n(x)$ for which

$$\frac{d}{dx}(T_n(x)) = 0 \qquad \text{at} \quad x = x_j, \quad 1 \leqslant j \leqslant N-1. \tag{43}$$

The pressure only occurs as a gradient in the momentum equation and, since this equation is collocated at the interior Chebyshev–Gauss–Lobatto nodes, the modes defined by (43) are termed spurious because they have no effect on the velocity. When $k = 0$ there is one spurious mode $T_N(x)$. Further, the constant mode $T_0(x)$ has no effect on the velocity since it represents the mean value of the pressure. Any solution procedure for (39)–(41) must take proper account of these modes; otherwise the numerical solution will be polluted. Spurious pressure modes were first characterized mathematically by Bernardi, Maday, and Métivet [6].

In Section 4 we assumed that u, v, and p belonged to the same space $\mathcal{P}_N$ of algebraic polynomials of degree less than or equal to N and therefore we expanded them in terms of truncated Chebyshev series of the same order. However, the approximation scheme will fail to determine a unique pressure p_N because of the rank deficiency of the system (39)–(41) when $k = 0$. We are, in effect, seeking to determine the pressure in the wrong approximation space. The velocity and pressure spaces must satisfy a compatibility condition which is equivalent to the Babuška–Brezzi condition in finite element theory. Therefore, in order to have a well-posed problem we must find a solution p_N in a suitably defined restricted subspace $\mathcal{Q}_N$ of $\mathcal{P}_N$. We define $\mathcal{Q}_N$ to be the subspace of $\mathcal{P}_N$ which is orthogonal to the linear subspace spanned by the constant and spurious pressure modes. We must therefore determine p_N in $\mathcal{Q}_N$ in order to satisfy the compatibility condition.

The linear system (39)–(41) for the pressure values p_j, $0 \leqslant j \leqslant N$, may be written as

$$A\mathbf{p} = \mathbf{b}, \tag{44}$$

where A is a matrix of order $N+1$ and rank $N-1$ when $k = 0$. Direct methods can be used to solve systems of the form (44) even when A is singular. Provided that the system is consistent then it can be solved using Gaussian elimination with the help of natural rounding error. Schumack, Schultz, and Boyd [27] use standard matrix solvers to obtain solutions to singular formulations. Bernardi, Canuto and Maday [5] show that the existence of spurious pressure modes does not pollute the velocity solution. However, since the gradient of the spurious pressure modes vanishes only at the collocation points these modes have no influence and hence no polluting effect on the pressure gradient at these points. For this reason the pressure gradient is "good" only at the collocation points. However, at points other than collocation points, the presence of spurious modes will pollute the pressure gradient. In order to obtain an unpolluted pressure one has to extract, using some sort of filtering technique, that part of the computed pressure which is orthogonal to the space spanned by the spurious modes.

An alternative way of finding a solution in $\mathcal{Q}_N$ is to augment the system (44) with the conditions which set the constant and spurious modes to zero, i.e.,

$$\hat{p}_0 = 0, \qquad \hat{p}_N = 0, \tag{45}$$

and then perform a SVD on the augmented system. In terms of the nodal pressure values we may write (45) in the form

$$\tfrac{1}{2}p_0 + p_1 + \cdots + p_{N-1} + \tfrac{1}{2}p_N = 0, \tag{46}$$

$$\tfrac{1}{2}p_0 - p_1 + \cdots - p_{N-1} + \tfrac{1}{2}p_N = 0. \tag{47}$$

We write the augmented system as

$$\tilde{A}\mathbf{p} = \tilde{\mathbf{b}}, \tag{48}$$

where $\tilde{A}$ is a $(N+3)\times(N+1)$ matrix and $\tilde{\mathbf{b}}$ is a vector obtained by adding two zero rows to $\mathbf{b}$. There exists orthogonal matrices Q and R of order $(N+3)\times(N+3)$ and $(N+1)\times(N+1)$, respectively, whose columns comprise the left and right singular vectors of $\tilde{A}$, respectively, such that

$$\tilde{A} = QDR^{\mathrm{T}}, \qquad D = \begin{pmatrix} \hat{D} \\ 0 \end{pmatrix},$$

where $\hat{D} = \mathrm{diag}(\lambda_1, \ldots, \lambda_{N+1})$ is the diagonal matrix containing the non-zero singular values of $\tilde{A}$. (See Golub and Van Loan [16], for example). In view of this decomposition we may write (48) in the form

$$QDR^{\mathrm{T}}\mathbf{p} = \tilde{\mathbf{b}},$$

which after premultiplication by Q^{T} gives

$$DR^{\mathrm{T}}\mathbf{p} = Q^{\mathrm{T}}\tilde{\mathbf{b}}. \tag{49}$$

This is a consistent system of equations for $\mathbf{p}$, provided that $\mathbf{q}_i^{\mathrm{T}}\tilde{\mathbf{b}} = 0$ for $i = N+2$, $N+3$, where $\mathbf{q}_i$ denotes the ith column of Q. Therefore the system is solvable, provided that the right-hand side vector $\tilde{\mathbf{b}}$ is orthogonal to the space spanned by the left singular vectors of $\tilde{A}$ corresponding to the two zero singular values. This is precisely the space spanned by the spurious pressure modes. These conditions are similar to the solvability conditions derived by Sani *et al.* [26] for finite element approximations to the incompressible Navier–Stokes equations. In some way these two sets of conditions must be equivalent since they have the same effect, namely, that they ensure that mass is conserved globally and that the pressure does not contain a component in the space spanned by the spurious pressure modes. Therefore, if we define $\hat{Q}$ to be the leading $(N+3)\times(N+1)$ submatrix of Q then p can be determined from

$$\mathbf{p} = R\hat{D}^{-1}\hat{Q}^{\mathrm{T}}\tilde{\mathbf{b}}. \tag{50}$$

Thus at the end of the projection step of the explicit algorithm the velocity field satisfies globally the incompressibility constraint and the no-slip boundary conditions. Furthermore, the pressure is free from spurious and constant modes.

For non-periodic problems in two dimensions there are seven spurious pressure modes, as well as the constant one, when a collocation grid composed of the Cartesian product of the Chebyshev–Gauss–Lobatto nodes is used (Bernardi, Canuto, and Maday [5]). If $\Omega = [-1, 1]\times[-1, 1]$ these modes are defined specifically by

(i) $T_N(x)$, $T_N(y)$, $T_N(x)\,T_N(y)$,

(ii) $(1 \pm x)\,T'_N(x)(1 \pm y)\,T'_N(y)$.

The gradient of the modes in (i) vanishes at the interior Chebyshev–Gauss–Lobatto points. The modes in (ii) are referred to as the corner modes since they vanish at all interior and boundary Chebyshev–Gauss–Lobatto points, except at one corner. In addition the gradient of these modes vanishes at all nodes except those which lie on the two straight lines which do not form the corner. Therefore the spurious and constant pressure modes span a subspace of dimension 8.

An important point to note here is that the value of the pressure at the four corner points does not affect the pressure values at the other collocation points. The pressure at the corners is determined by imposing the continuity equation at these points and eliminating the values of $\mathbf{v}^{n+1}$ which occur at the interior boundary collocation points using the discrete form of (24) and (25). This requires the values of the intermediate velocity at the interior boundary collocation points. The determination of the pressure proceeds as follows. First, we impose the continuity equation at all collocation points to obtain a system of the form (44) for the pressure values where A is now a matrix of order $M = (N+1)^2$ and rank $M-4$. Second, we augment this system by the algebraic equations which set the spurious and constant modes to zero, i.e.,

$$\hat{p}_{0,0} = \hat{p}_{N,0} = \hat{p}_{0,N} = \hat{p}_{N,N} = 0. \tag{51}$$

Finally, we perform as SVD on the augmented coefficient matrix and determine the pressure as in the 1D case. At the end of this process the pressure is orthogonal to the subspace spanned by the spurious and constant modes and the velocity field is divergence-free at all boundary and interior collocation points.

The truncated influence matrix of Farcy and Alziary de Roquefort [12] is shown to be regular even though the original influence matrix has rank $M-8$. However, Farcy and Alziary de Roquefort state that there is no physical justification for this. Their method requires the solution of M Stokes problems in a pre-processing stage. The amount of work involved here can be substantial, particularly if M is large. An iterative method is necessary to ensure that the velocity field is sufficiently divergence-free. The oscillations

in the solution are removed by filtering out the spurious pressure modes at the end of each time step. In contrast the method proposed in the present paper suitably modifies the algebraic system for the pressure so that the pressure is orthogonal to the space spanned by the spurious modes.

Schumack, Schultz, and Boyd [27] have shown that there are alternative ways of eliminating spurious pressure modes in spectral methods when the Stokes equations are solved directly without resorting to staggered grids. They obtain a nonsingular system in a number of ways, including the application of the normal momentum equation on the boundary, the use of a lower order basis for the pressure approximation and over-determination. They solve a weak formulation of the problem and, because of the choice of pressure space used, a globally divergence-free velocity field is not obtained. Our scheme produces a velocity field which is globally divergence-free and not just at the collocation points. The space which we have chosen for the pressure has been shown to result in a well-posed problem for Stokes flow and guarantees spectral accuracy of the approximations ([5]). Thus the optimality of the approximations used in the present paper is the main difference between the two approaches and the existence of a formal error analysis puts the proposed method on a firm theoretical basis.

Although the modified pressure equation (44) is singular it may still be solved by standard Gaussian elimination techniques because roundoff errors result in small but nonzero pivots. The pressure gradient field is accurate at the collocation points which therefore gives an accurate velocity field. The pressure field itself is polluted by the spurious pressure modes as described above. If accurate pressure values are required, the spurious modes may be removed by subsequent filtering. A straightforward way of filtering is to take the discrete transform of the pressure field, set the appropriate coefficients to zero, and transform back.

When using our scheme to obtain steady state results, the PPE operator is identical at each time step. For problems taking more than a trivial number of time steps, it is more efficient to multiply by the inverse of the PPE operator rather than retain the LU decomposition and perform a forward and back substitution at each time step.

The condition number of the discrete PPE operator precludes the use of its inverse, but the SVD with the addition of zero pressure mode conditions gives an accurate inverse which may be stored and used at each time step. In this case it is unnecessary to filter the pressure field. The initial computational effort in performing the SVD and calculating the inverse is more than compensated by the saving accumulated at each subsequent time step.

Our SVD scheme sets the spurious pressure modes to zero before solving the PPE, therefore giving a nonsingular, moderately conditioned system. It does not remove solvability constraints on the velocity field in order that the PPE is consistent and these constraints are an area for further investigation. This issue is addressed in the finite element context by Sani *et al.* [26]. For the examples given in this paper, the PPE is always consistent.

6. A SPLITTING SCHEME FOR THE NAVIER–STOKES EQUATIONS

The time splitting scheme for the Navier–Stokes equations (1)–(2) is a straightforward extension of that for the Stokes problem.

TRANSIENT NAVIER–STOKES SCHEME. *Stage* A.

$$\frac{\mathbf{v}^* - \mathbf{v}^n}{\Delta t} = [\nu \nabla^2 \mathbf{v} - \mathbf{v} \cdot \nabla \mathbf{v}]^n. \tag{52}$$

Stage B.

$$\frac{\mathbf{v}^{n+1} - \mathbf{v}^*}{\Delta t} = -\nabla p^n \tag{53}$$

$$\nabla \cdot \mathbf{v}^{n+1} = 0 \tag{54}$$

$$\mathbf{v} = 0 \qquad \text{on the no-slip boundary.} \tag{55}$$

The stability of the scheme is governed by the viscous term $\nu \Delta t \nabla^2 \mathbf{v}$ for small values of the Reynolds number. When the problem is convection dominated the stability of the scheme is governed by the usual CFL condition.

7. A SPLITTING SCHEME FOR NON-NEWTONIAN FLOWS

The equations governing the transient flow of an incompressible non-Newtonian fluid of Oldroyd B type are

$$\rho\left(\frac{\partial \mathbf{v}}{\partial t} + \mathbf{v} \cdot \nabla \mathbf{v}\right) = -\nabla p + \nabla \cdot \mathbf{T}, \tag{56}$$

$$\nabla \cdot \mathbf{v} = 0, \tag{57}$$

$$\mathbf{T} + \lambda_1 \overset{\nabla}{\mathbf{T}} = 2\eta(\mathbf{d} + \lambda_2 \overset{\nabla}{\mathbf{d}}), \tag{58}$$

where $\mathbf{T}$ is the extra-stress tensor, $\mathbf{d} = \frac{1}{2}(\nabla \mathbf{v} + \nabla \mathbf{v}^{\mathrm{T}})$ is the rate of deformation tensor, ρ is the density, η is the viscosity, and λ_1 and λ_2 are characteristic relaxation and retardation times for the fluid, respectively. In the following we choose λ_2 according to the relationship $\lambda_2 = \frac{1}{5}\lambda_1$. The upper-convected derivative of $\mathbf{T}$ is defined by

$$\overset{\nabla}{\mathbf{T}} = \frac{\partial \mathbf{T}}{\partial t} + \mathbf{v} \cdot \nabla \mathbf{T} - \nabla \mathbf{v} \cdot \mathbf{T} - \mathbf{T} \cdot (\nabla \mathbf{v})^{\mathrm{T}}. \tag{59}$$

We may decompose the extra-stress tensor $\mathbf{T}$ into its viscoelastic and viscous parts as

$$\mathbf{T} = \tau + 2\eta_2 \mathbf{d}, \tag{60}$$

where the viscoelastic part, τ, satisfies

$$\tau + \lambda_1 \overset{\nabla}{\tau} = 2\eta_1 \mathbf{d}. \tag{61}$$

The constants η_1 and η_2 are defined by the relationships

$$\eta = \eta_1 + \eta_2, \qquad \lambda_2 = \frac{\eta_2}{\eta}\lambda_1.$$

The time splitting scheme for the solution of non-Newtonian flow problems follows closely the explicit scheme we have already described for Newtonian flows. However, for non-Newtonian problems the constitutive equation (58) must also be advanced in time in order for the components of extra-stress to be updated at the new time level. Due to the complicated form of the constitutive relationship this equation is treated explicitly using the forward Euler method.

TRANSIENT NON-NEWTONIAN SCHEME. *Stage* A.

$$\frac{\lambda_1}{\Delta t}(\tau^{n+1} - \tau^n) = [2\eta_1 \mathbf{d} - \tau - \lambda_1[\mathbf{v}\cdot\nabla\tau - \{\nabla\mathbf{v}\cdot\tau\} - \{\tau\cdot(\nabla\mathbf{v})^{\mathrm{T}}\}]]^n. \tag{62}$$

Stage B.

$$\frac{\rho}{\Delta t}(\mathbf{v}^* - \mathbf{v}^n) = [\nabla\cdot\tau + \eta_2\nabla^2\mathbf{v} - \rho\mathbf{v}\cdot\nabla\mathbf{v}]^n. \tag{63}$$

Stage C.

$$\frac{\rho}{\Delta t}(\mathbf{v}^{n+1} - \mathbf{v}^*) = -\nabla p^n \tag{64}$$

$$\nabla\cdot\mathbf{v}^{n+1} = 0 \tag{65}$$

$$\mathbf{v} = 0 \qquad \text{on the no-slip boundary.} \tag{66}$$

The constitutive relationship is treated explicitly in Stage A over the whole time step. The determination of the pressure and the treatment of the incompressibility constraint are treated again using the method of Ku, Taylor, and Hirsh [21] to modify the discrete derivative operators in the derivation of the pressure problem.

8. NUMERICAL RESULTS

Poiseuille Flow in a 2D Planar Channel

We consider the flow of an Oldroyd B fluid in the planar channel $-1 \leqslant x \leqslant 1$, $-1 \leqslant y \leqslant 1$ with entry and exit sections at $x = -1$ and $x = 1$, respectively. The walls $y = \pm 1$ are no-slip boundaries. We assume Poiseuille flow at entry with a mean flow rate of unity which implies that for $t \geqslant 0$, $-1 \leqslant y \leqslant 1$,

$$u(-1, y, t) = \tfrac{3}{4}(1 - y^2), \quad v(-1, y, t) = 0.$$

The entry conditions for stress are obtained from (58) and (59) by setting all the x-derivatives to zero and also $v = 0$. Thus at entry for $t \geqslant 0$, $-1 \leqslant y \leqslant 1$,

$$T_{xx}(-1, y, t) = \tfrac{9}{2}\eta(\lambda_1 - \lambda_2)\, y^2,$$
$$T_{xy}(-1, y, t) = -\tfrac{3}{2}\eta y, \qquad T_{yy}(-1, y, t) = 0.$$

At exit we impose the same parabolic profile as that specified at entry. Of course, the steady state solution is also fully developed and repeats the entry profile at any cross section of the channel. In our calculations we specify the values of the flow variables in the interior of the domain to be zero at time $t = 0$. The algorithm is then allowed to run until the steady state solution is reached. The tolerance for all the numerical examples is that the relative error of all the variables is less than 10^{-6}. A smaller value for the tolerance was also used to ensure that steady state is reached.

Results for the 2D channel flow obtained on an 8×8 mesh are shown in Table I for different values of λ_1. In the absence of inertia it is possible to converge to a steady state solution in far fewer iterations using the method of false transients. This method was first introduced by Mallinson and De Vahl Davis [22]. They observed that a lower time step restriction is generally needed when solving a system of time-dependent equations than when solving a single equation. However, instabilities which may occur if this stability condition is violated may be controlled if different time steps are used for the separate equations. In the present context the method essentially uses different time steps for the

TABLE I

Oldroyd-B Results for 2D Channel Flow on an 8×8 Mesh

λ_1	ρ	Δt	*nsteps*
0.0	1.0	1.0 − 3	407
0.1	1.0	1.0 − 3	1247
0.1	1.0 + 2	1.0 − 1	467
1.0	1.0	1.0 − 3	16466
1.0	1.0 + 2	1.0 − 1	681

TABLE II

Time Step and Convergence Speed for the Newtonian 2D Regularized Driven Cavity for a 24×24 Mesh (Convergence Criterion 10^{-6})

Re	ν	Δt	Δt/Re	*nsteps*
0	1.0 + 0	2.5 − 5	—	4959
1	1.0 + 0	2.5 − 5	2.5 − 5	4959
100	1.0 − 2	2.5 − 3	2.5 − 5	5091
200	5.0 − 3	5.0 − 3	2.5 − 5	4933
400	2.5 − 3	1.0 − 2	2.5 − 5	3955
1000	1.0 − 3	2.0 − 2	2.5 − 5	3709
2000	5.0 − 4	2.0 − 2	1.0 − 5	7154

momentum and constitutive equations. The effective time step for the momentum equation is $\Delta t/\rho$ so that for $\rho > 1$ we effectively use a smaller time step for the momentum equation than for the constitutive equation. This has a dramatic effect on the number of iterations required to reach steady state and a more marked reduction is achieved for higher values of λ_1.

Flow in a Regularized Driven Square Cavity

We consider the flow of a Newtonian fluid in the regularized driven square cavity $0 \leqslant x \leqslant 1$, $0 \leqslant y \leqslant 1$ as used by Demaret and Deville [10] and Shen [28]. In this problem the flow is driven by a theoretical horizontal

TABLE III

Properties of Vortices for the Newtonian 2D Regularized Driven Cavity

Re Grid	Reference	Primary	Secondary bottom right	Secondary bottom left	Secondary top left
0	Present	−8.3618 − 2	1.6600 − 6	1.6600 − 6	—
24 × 24		(0.500, 0.778)	(0.962, 0.038)	(0.038, 0.038)	
1	Present	−8.3617 − 2	1.6702 − 6	1.6500 − 6	—
24 × 24		(0.500, 0.778)	(0.962, 0.038)	(0.038, 0.038)	
100	Present	−8.3627 − 2	4.8040 − 6	1.2312 − 6	—
24 × 24		(0.598, 0.757)	(0.952, 0.048)	(0.038, 0.038)	
100	Shen	−8.368 − 2	4.6676 − 6	1.3987 − 6	—
17 × 17		(0.609, 0.750)	(0.953, 0.047)	(0.031, 0.031)	
200	Present	−8.4504 − 2	3.3750 − 5	1.7731 − 6	—
24 × 24		(0.621, 0.691)	(0.929, 0.084)	(0.038, 0.038)	
400	Present	−8.5877 − 2	2.5487 − 4	5.7072 − 6	—
24 × 24		(0.573, 0.621)	(0.902, 0.113)	(0.048, 0.038)	
400	Shen	−8.584 − 2	1.9774 − 4	6.3146 − 6	—
17 × 17		(0.578, 0.625)	(0.922, 0.094)	(0.031, 0.047)	
1000	Present	−8.7128 − 2	9.8882 − 4	8.6133 − 5	—
24 × 24		(0.549, 0.573)	(0.870, 0.113)	(0.071, 0.071)	
1000	Shen	−8.719 − 2	5.6762 − 4	8.2841 − 5	—
25 × 25		(0.547, 0.578)	(0.922, 0.094)	(0.078, 0.063)	
2000	Present	−8.7613 − 2	1.5964 − 3	3.6334 − 4	1.0133 − 4
24 × 24		(0.525, 0.549)	(0.854, 0.113)	(0.084, 0.098)	(0.038, 0.887)
2000	Present	−8.7513 − 2	1.5833 − 3	3.5541 − 4	7.3403 − 5
32 × 32		(0.525, 0.549)	(0.854, 0.098)	(0.084, 0.098)	(0.038, 0.887)
2000	Demaret	−8.7836 − 2	1.6062 − 3	3.5293 − 4	1.0251 − 4
25 × 25	Deville	(0.529, 0.553)	(0.850, 0.103)	(0.087, 0.094)	(0.041, 0.891)
2000	Shen	−8.762 − 2	8.0667 − 4	3.1772 − 4	1.4497 − 5
25 × 25		(0.531, 0.547)	(0.922, 0.094)	(0.078, 0.094)	(0.031, 0.092)
2000	Shen	−8.776 − 2	8.0841 − 4	3.5432 − 4	1.7143 − 5
33 × 33		(0.531, 0.547)	(0.922, 0.094)	(0.094, 0.094)	(0.031, 0.092)
4500	Present	−8.7979 − 2	2.0700 − 3	7.9866 − 4	6.8318 − 4
32 × 32		(0.525, 0.537)	(0.817, 0.084)	(0.084, 0.121)	(0.071, 0.902)
4500	Demaret	−8.8756 − 2	2.1204 − 3	7.8872 − 4	6.3715 − 4
29 × 29	Deville	(0.521, 0.539)	(0.814, 0.082)	(0.081, 0.120)	(0.087, 0.915)
5000	Present	−8.7984 − 2	2.1168 − 3	8.4659 − 4	7.7873 − 4
32 × 32		(0.525, 0.537)	(0.808, 0.078)	(0.084, 0.121)	(0.078, 0.902)
5000	Shen	−8.803 − 2	7.7475 − 4	7.5268 − 4	6.7780 − 4
33 × 33		(0.516, 0.531)	(0.922, 0.094)	(0.094, 0.094)	(0.078, 0.092)

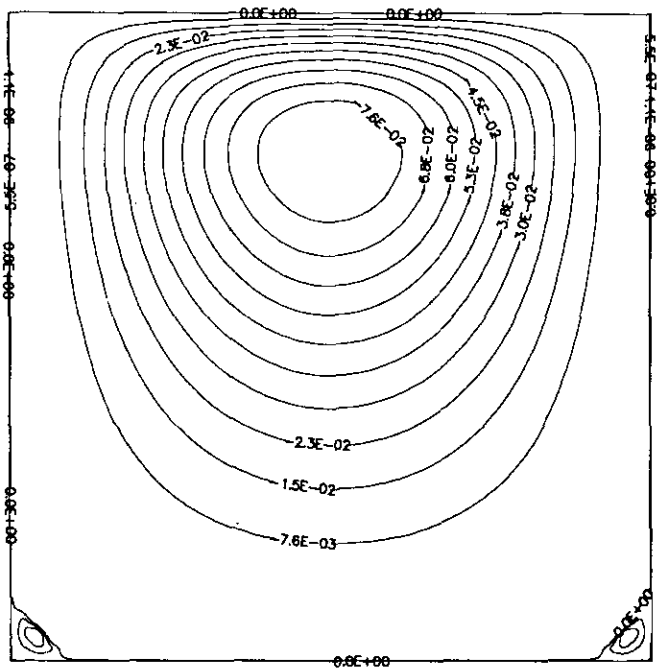

FIG. 1. Streamlines for the regularized driven cavity, Re = 0.

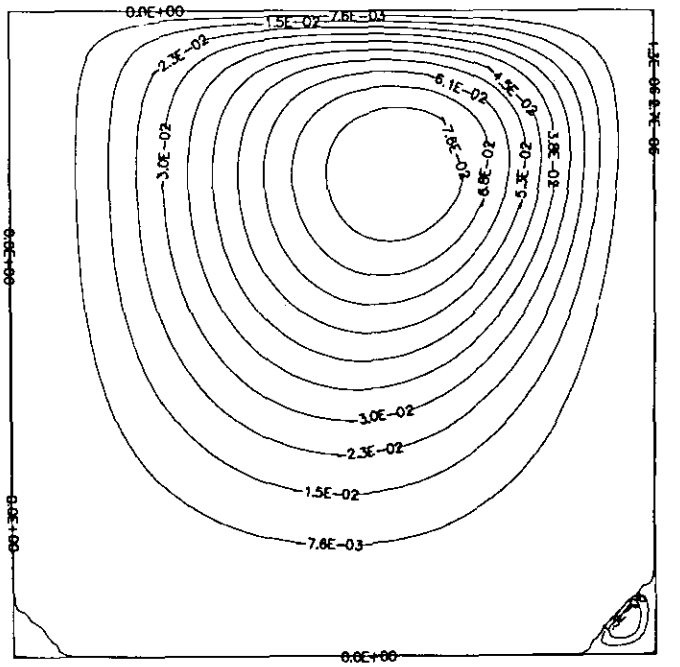

FIG. 3. Streamlines for the regularized driven cavity, Re = 100.

motion of the top lid of the cavity such that the horizontal velocity component there is given by $u(x, 1) = 16x^2(1-x)^2$ and the vertical component is zero. This velocity distribution removes the singularities at the top corners of the standard driven cavity and therefore preserves the high accuracy of the spectral space discretization. The boundary conditions on the other sides are zero velocity no-slip conditions.

Table II presents details of the time steps and convergence speed for the Navier–Stokes scheme for different Reynolds numbers on a 24×24 mesh. Inspection of (52) shows that the nonlinear term is multiplied by Δt while the

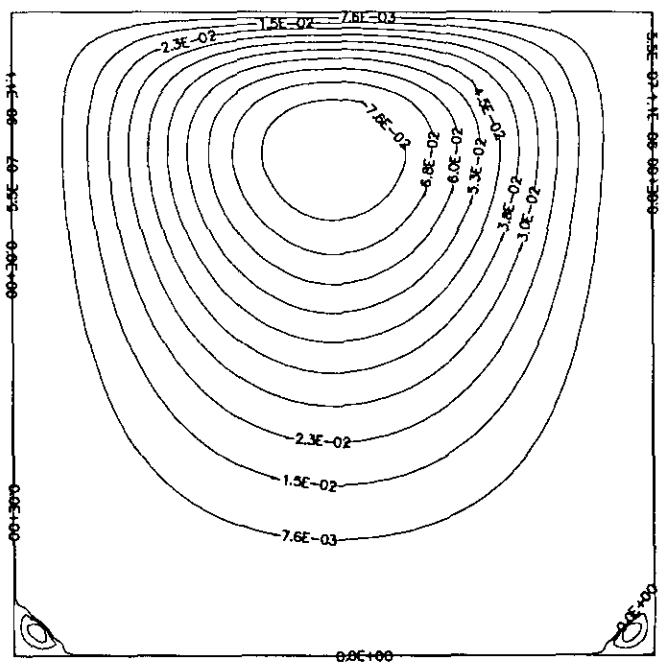

FIG. 2. Streamlines for the regularized driven cavity, Re = 1.

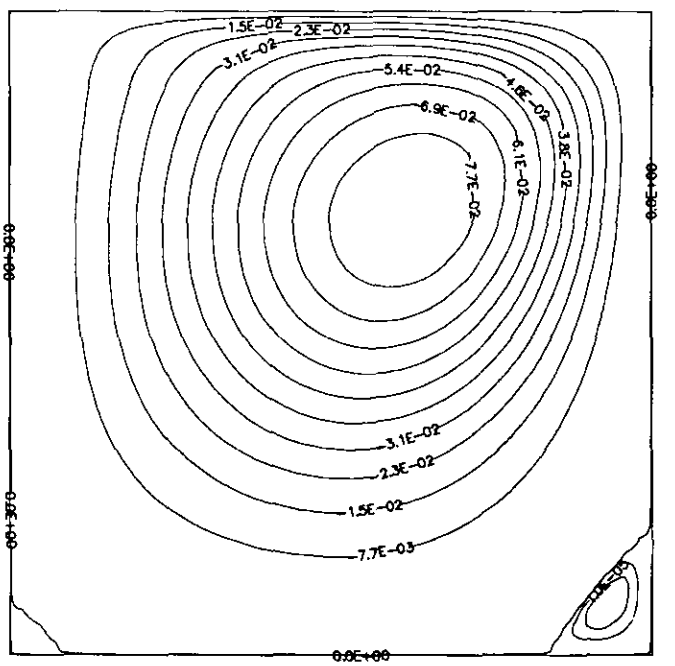

FIG. 4. Streamlines for the regularized driven cavity, Re = 200.

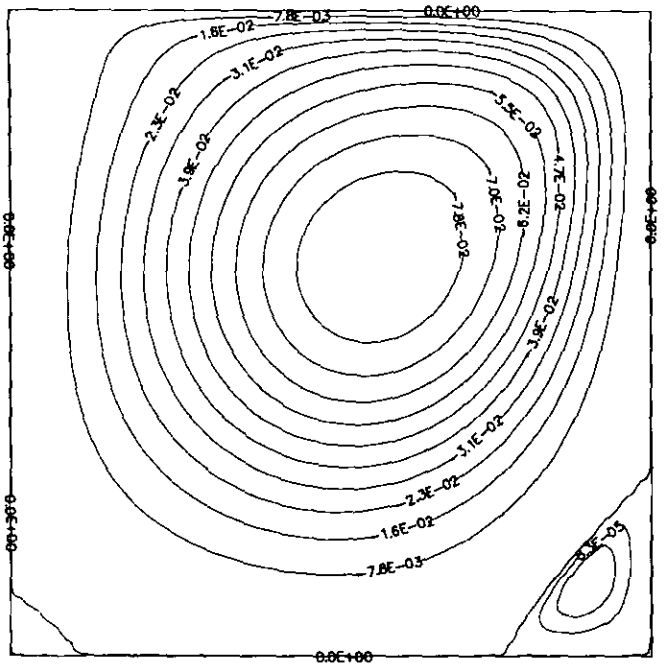

FIG. 5. Streamlines for the regularized driven cavity, Re = 400.

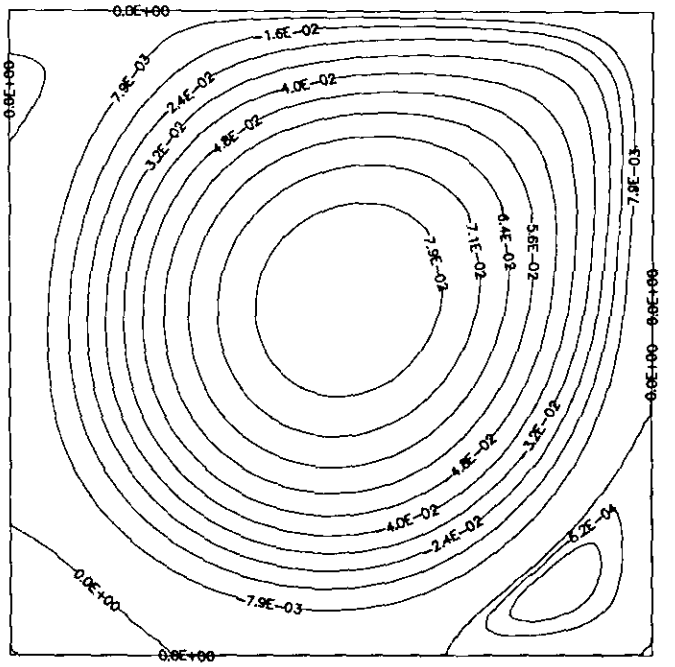

FIG. 7. Streamlines for the regularized driven cavity, Re = 2000.

viscous term is multiplied by $\nu\,\Delta t = \Delta t/\mathrm{Re}$ which is the factor that to a large extent governs the stability of the scheme. If the Reynolds number is increased by decreasing the kinematic viscosity ν, it may be seen that Δt may be increased accordingly in order to keep the term $\Delta t/\mathrm{Re}$ as large as possible, but within the stability limit. Thus a larger time step is permissible as the Reynolds number is increased and results in a large saving in the computer time required to reach steady state. The maximum time step which gave stability was obtained experimentally for each Reynolds number; for $\mathrm{Re} \leqslant 2000$ we need $\Delta t/\mathrm{Re} \leqslant 2.5 \times 10^{-5}$ for stability. At Re = 2000 a smaller value of $\Delta t/\mathrm{Re}$ is required

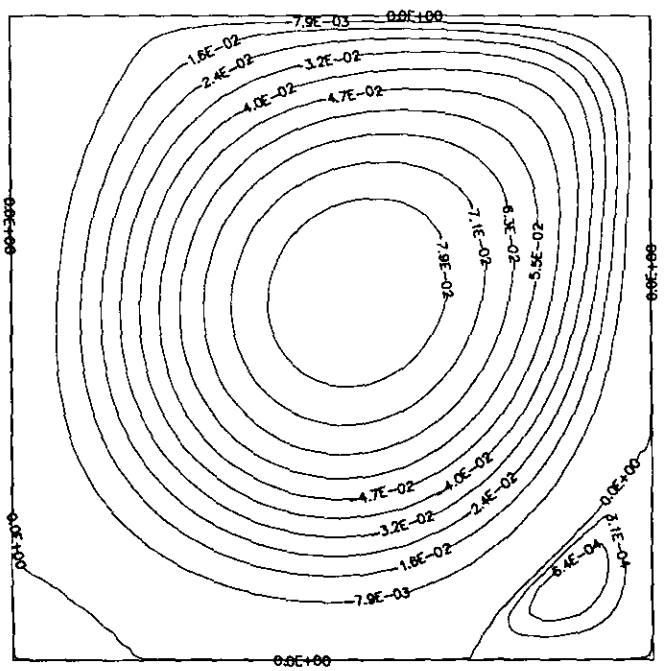

FIG. 6. Streamlines for the regularized driven cavity, Re = 1000.

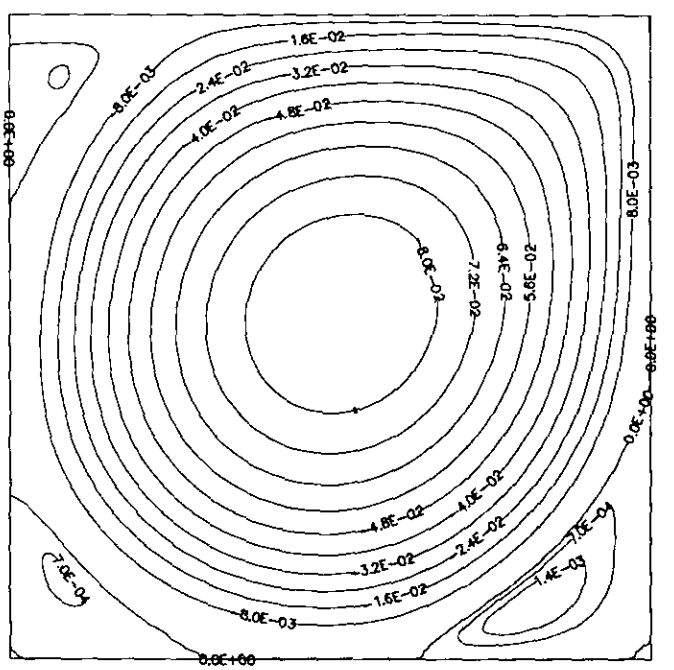

FIG. 8. Streamlines for the regularized driven cavity, Re = 5000.

which suggests that the convective term is now the main influence on the stability of the scheme.

Figures 1 to 8 show streamline contours for different values of the Reynolds number in the range 0 to 5000.

Table III gives a quantitative comparison of our present results with those obtained by Demaret and Deville [10] and Shen [28] for Reynolds numbers up to 5000. In general there is good agreement for the positions of primary and secondary vortices and the associated values of the stream function. For a Reynolds number of 2000 the results for the secondary bottom right and top left vortices agree with Demaret and Deville, whereas Shen predicts lower values of the stream function. Also, there appear to be typing errors in the values for the y-coordinate of the top left vortex in Shen's paper.

Our results indicate that weak tertiary vortices appear at the bottom right for $\mathrm{Re}=400$, at the bottom left for $\mathrm{Re}=1000$, and at the top right for $\mathrm{Re}=5000$.

Flow between Eccentrically Rotating Cylinders

We consider the flow of an upper-convected Maxwell fluid (UCM) between eccentrically rotating cylinders. The UCM model is obtained as a special case of the Oldroyd-B constitutive equation by setting $\lambda_2=0$. The flow geometry is shown in Fig. 9. The inner and outer cylinders are of radius R_J and R_B, respectively, with the distance between the centres of the cylinders given by e. The outer cylinder is kept at rest, while the inner cylinder is rotated at an angular velocity Ω. The eccentricity is defined by $\varepsilon=e/c$, where $c=R_B-R_J$ is known as the gap. The Deborah and Weissenberg numbers are non-dimensional elasticity parameters and for this flow they are defined by

$$\mathrm{De}=\lambda_1\Omega, \qquad \mathrm{We}=\lambda_1\Omega\frac{R_J}{c}.$$

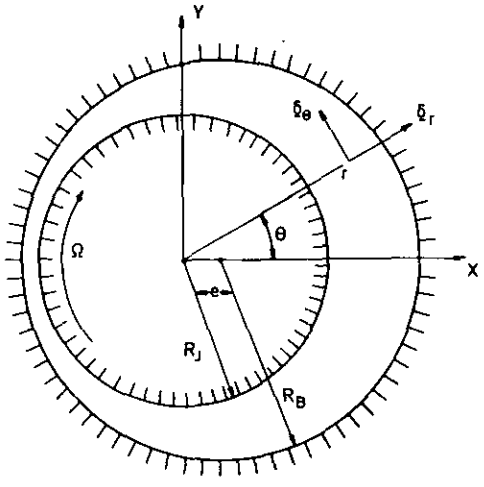

FIG. 9. Geometry of eccentric cylinder model.

TABLE IV

UCM Results for Eccentric Cylinder on an 8×8 Mesh with $D=0.03125$, $c=0.00004$, and $\varepsilon=0.1$

λ	ρ	Δt	*nsteps*	F_X	F_Y	C
0.0	1.0	5.0−10	641	0.0	4.50+4	6.12+0
1.0−6	2.0+3	1.0−6	683	7.52+0	4.50+4	6.12+0
1.0−5	2.0+3	1.0−6	600	7.52+1	4.50+4	6.12+0
1.0−4	2.0+3	1.0−6	2201	7.52+2	4.50+4	6.12+0
1.0−3	2.0+3	1.0−6	18802	7.37+3	4.41+4	6.12+0

The use of cylindrical bipolar coordinates enables the region between the cylinders to be mapped conformally onto a concentric geometry, where a Fourier–Chebyshev basis is used to approximate the flow variables. The cylindrical bipolar system (ξ,η) (see Fig. 10) is given by

$$x=\frac{a\sinh\xi}{\chi}, \qquad y=\frac{a\sin\eta}{\chi},$$

where $\chi=\cosh\xi+\cos\eta$ and a is a constant depending on ε, R_J, and R_B. The Stokes equations in terms of bipolar coordinates are given in Roberts *et al.* [25].

Numerical results are presented in Table IV for $\varepsilon=0.1$ on an 8×8 mesh and in Table V for $\varepsilon=0.5$ on a 12×12 mesh. In addition to parameters relating to the performance of the algorithm the couple and components of the force per unit length on the journal are also given. We see that by using the method of false transients for nonzero values of λ_1 we are able to use a time step that is at least 10^4 times the size of the time step required for the momentum equation. This enables greater efficiency when only the steady state solution is required. For nonzero values of λ_1 the horizontal load increases linearly with λ_1 and the resultant force no longer acts normal to the line joining the centres of the journal and the bearing.

The physical relaxation times for oil are in the range 10^{-6}–10^{-5}. We have obtained results for considerably higher values of λ_1 without noticing any nonlinear effects. In

TABLE V

UCM Results for Eccentric Cylinder on a 12×12 mesh with $D=0.03125$, $c=0.00004$, and $\varepsilon=0.5$

λ	ρ	Δt	*nsteps*	F_X	F_Y	C
0.0	1.0	3.0−11	4622	0.0	2.30+5	9.25+0
1.0−6	1.0+4	3.0−7	4609	4.48+1	2.30+5	9.24+0
1.0−5	1.0+5	3.0−6	4609	4.48+2	2.31+5	9.24+0
1.0−4	1.0+6	3.0−5	4738	4.48+3	2.31+5	9.24+0
1.0−3	1.0+6	3.0−5	4558	4.18+4	2.24+5	9.18+0
1.5−3	1.0+6	3.0−5	4585	5.90+4	2.18+5	9.12+0
2.0−3	1.0+6	3.0−5	19414	7.41+4	2.11+5	9.07+0

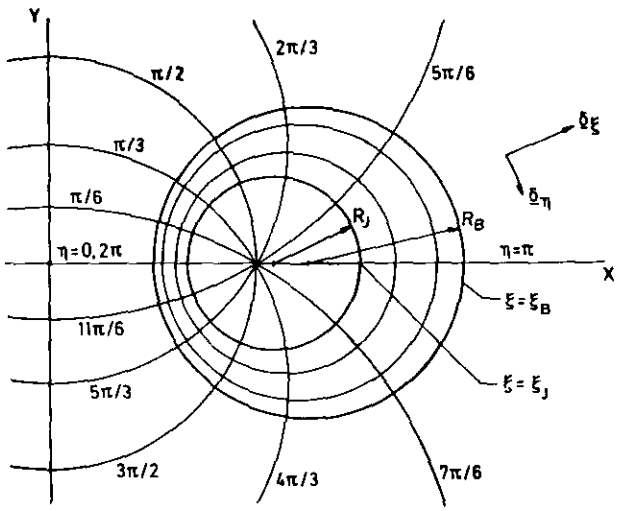

FIG. 10. Bipolar coordinate system.

the example with $\varepsilon = 0.5$ the Weissenberg number in the region of smallest gap is approximately 780. These physical choices of the parameters are a severe test for any numerical algorithm. We obtain velocity fields that are divergence-free to machine accuracy at the collocation points as a result of the projection method that we use in our numerical scheme.

Beris, Armstrong, and Brown [1–4] have calculated the viscoelastic flow between eccentrically rotating cylinders for a variety of constitutive relations using both finite element and spectral/finite element methods. The use of the latter method for the UCM model alleviated numerical oscillations that were present in the earlier finite element work and resolved the stress boundary layers that exist for high elasticity, as measured by the Deborah number. The use of Fourier expansion functions in the azimuthal direction enabled solutions to be calculated for higher values of De than were possible using the finite element method. However, the method was less successful at predicting the flow and stress fields for high De at large eccentricity. The use of the fully spectral discretization described in this paper has circumvented this difficulty and enabled solutions to be obtained for large values of the relaxation time.

9. CONCLUSIONS

In this paper we consider algorithms for the transient simulation of incompressible Newtonian and non-Newtonian flows. Particular attention is given to the satisfaction of the incompressibility constraint and the determination of the pressure when spectral expansions are used to approximate the flow variables. If the steady state solution is required we advocate the use of the method of false transients which greatly reduces the amount of computational effort required by using a much larger time step for the constitutive equation.

Implicit and explicit schemes are described for solving a one-dimensional Stokes problem which is a model which possesses the same computational difficulties as those associated with the Navier–Stokes equations when written in primitive variable form. A projection method is used to ensure that the velocity field is divergence-free at the end of each time step. An algorithm of Ku, Taylor, and Hirsh [21] circumvents the need to impose values of the intermediate velocity components at the boundary. The algebraic system for the pressure is closed by imposing the continuity equation at the boundary collocation points in addition to the interior points. The resulting system is singular due to the presence of spurious pressure modes. This difficulty is overcome by seeking the pressure in a suitably defined restricted subspace of the space of algebraic polynomials of given degree which is orthogonal to these modes. This is achieved computationally using the singular value decomposition in which rows of the pressure system which correspond to singular values are replaced by conditions which set these modes to zero. At the end of each time step the pressure is free from spurious modes, the velocity field is divergence-free at all boundary and interior collocation points and the no-slip boundary conditions are satisfied. In addition, for problems defined in cartesian domains the velocity approximation is globally divergence-free.

The numerical results demonstrate that spectral methods are capable of solving incompressible flow problems of practical importance for realistic values of the material parameters.

ACKNOWLEDGMENTS

This work was partly funded by Shell Research Ltd., Thornton, UK. We also thank a reviewer for suggesting several improvements to the manuscript.

REFERENCES

1. A. Beris, R. C. Armstrong, and R. A. Brown, *J. Non-Newtonian Fluid Mech.* **13**, 109 (1983).
2. A. N. Beris, R. C. Armstrong, and R. A. Brown, *J. Non-Newtonian Fluid Mech.* **16**, 141 (1984).
3. A. N. Beris, R. C. Armstrong, and R. A. Brown, *J. Non-Newtonian Fluid Mech.* **19**, 323 (1986).
4. A. N. Beris, R. C. Armstrong, and R. A. Brown, *J. Non-Newtonian Fluid Mech.* **22**, 129 (1987).
5. C. Bernardi, C. Canuto, and Y. Maday, *C.R. Acad. Sci. Paris Ser. I* **303**, 971 (1986).
6. C. Bernardi, Y. Maday, and B. Metivet, *C.R. Acad. Sci. Paris Ser. I* **303**, 163 (1986).
7. C. Canuto, M. Y. Hussaini, A. Quarteroni, and T. A. Zang, *Spectral Methods in Fluid Dynamics* (Springer-Verlag, Berlin, 1987).
8. A. J. Chorin, *J. Comput. Phys.* **2**, 12 (1967).
9. A. J. Chorin, *Math. Comput.* **22**, 745 (1968).

10. P. Demaret and M. Deville, *J. Comput. Phys.* **95**, 359 (1991).
11. M. Deville, L. Kleiser, and F. Montigny-Rannou, *Int. J. Numer. Methods Fluids* **4**, 1149 (1984).
12. A. Farcy and T. Alziary de Roquefort, *Comput. & Fluids* **16**, 459 (1988).
13. M. Fortin, R. Peyret, and R. Temam, *J. Méc.* **10**, 357 (1971).
14. P. M. Gresho and R. L. Sani, *Int. J. Numer. Methods Fluids* **7**, 1111 (1987).
15. P. M. Gresho, Preprint UCRL-JC-105019; *Adv. in Appl. Math.* submitted.
16. G. H. Golub and C. F. van Loan, *Matrix Computations* (The Johns Hopkins Univ. Press, Baltimore, 1983).
17. D. Gottlieb and S. A. Orszag, *Numerical Analysis of Spectral Methods: Theory and Applications* (SIAM-CBMS, Philadelphia, 1977).
18. J. C. Heywood and R. Rannacher, *SIAM J. Numer. Anal.* **23**, 750 (1986).
19. L. Kleiser and U. Schumann, in *Proceedings, 3rd GAMM Conf. Numerical Methods in Fluid Mechanics*, edited by E. H. Hirschel (Vieweg, Braunschweig, 1980).
20. L. Kleiser and U. Schumann, in *Spectral Methods for Partial Differential Equations*, edited by R. G. Voigt, D. Gottlieb, and M. Y. Hussaini (SIAM-CBMS, Philadelphia, 1984).
21. H. C. Ku, T. D. Taylor, and R. S. Hirsh, *Comput. & Fluids* **15**, 195 (1987).
22. G. D. Mallinson and G. de Vahl Davis, *J. Comput. Phys.* **12**, 435 (1973).
23. S. A. Orszag, M. Israelli, and M. O. Deville, *J. Sci. Comput.* **1**, 75 (1986).
24. R. Peyret and T. D. Taylor, *Computational Methods in Fluid Flow* (Springer-Verlag, Berlin, 1984).
25. G. W. Roberts, A. R. Davies, and T. N. Phillips, *Int. J. Numer. Methods Fluids* **13**, 217 (1991).
26. R. L. Sani, P. M. Gresho, R L. Lee, and D. F. Griffiths, *Int. J. Numer. Methods Fluids* **1**, 17 (1981).
27. M. R. Schumack, W. W. Schultz, and J. P. Boyd, *J. Comput. Phys.* **94**, 30 (1991).
28. J. Shen, *J. Comput. Phys.* **95**, 228 (1991).
29. A. Solomonoff and E. Turkel, *J. Comput. Phys.* **81**, 239 (1989).
30. R. Temam, *Bull. Soc. Math. France* **96**, 115 (1968).
31. R. Temam, *Navier–Stokes Equations* (North-Holland, Amsterdam, 1977).
32. N. N. Yanenko, *The Method of Fractional Steps* (Springer-Verlag, New York, 1971).